The possibilities of remote sensing of chemical warfare agents with a CO_2 lidar by differential absorption method

S.M. Bobrovnikov,[1] P.P. Geiko,[2] and I.S. Popov[2]

[1]V.E. Institute of Atmospheric Optics,
Siberian Branch of the Russian Academy of Sciences, Tomsk
[2]Institute of Monitoring of Climatic and Ecological Systems,
Siberian Branch of the Russian Academy of Sciences, Tomsk

The possibilities of remote sensing of chemical warfare agents by the differential absorption method are analyzed. The CO_2 laser emission lines suitable for sensing chemical warfare agents with accounting for disturbing absorption by water vapor were chosen. The detection range of chemical warfare agents is obtained for a lidar based on CO_2 laser. Factors influencing upon the sensing range have been analyzed.

Introduction

The problem of high-precision remote detection and identification of toxicity sources can be solved most effectively on the basis of lidar technologies well showing themselves in environmental monitoring. At present, the list of chemical warfare agents (CWA) includes tens of names. Each such agent is highly toxic and capable to cause lethal outcome or human health hazard. The most common among them are sarin, soman, tabun, cyclosarin, VX, and lewisite.

As is known, the most sensitive are methods of the remote monitoring of atmospheric components, based on the effect of selective absorption of optical radiation. Lidar responses, caused by reflection of laser pulses with close wavelengths λ_1 and λ_2 by atmospheric aerosols or topographic objects, attenuate similarly in clear air. However, when coming into a contaminated cloud, the response at λ_1 attenuates more than those at λ_2. Joint processing of the signals allows calculation of contaminant concentrations at known absorption coefficients for the above wavelengths. High signal intensity allows one to obtain on-line data on spatiotemporal distribution of contaminants in the atmosphere due to rapid scanning of a monitored object. However, some difficulties appear, connected with search for absorption bands or individual lines in the spectrum of the contaminant to be detected.

There are intensive rovibrational absorption bands of a number of CWA within the 9–11 μm region.[1,2] The laser, suitable for detecting such gases, is to have a high peak power, sufficiently narrow spectral width, short pulse length at small angular divergence of radiation, and comparatively high pulse repetition rate. The TEA–CO_2 laser answers these requires.[3,4]

Choice of sensing lines and physical principles

Along with CWA, there are background gases in the atmosphere (H_2O vapors, CO_2, etc.), which interfere the choice of optimal sensing wavelengths. Using the spectral line atlas,[5] interfering absorption of CWA by background gases was calculated, first of all for CO_2 and H_2O, since the absorption by water vapor within the 9–11 μm region essentially influences the choice of a couple of lines for sensing. Spectral data on CWA have been taken from Ref. 1. Superimposing the transmission spectrum of H_2O and CO_2 vapors on those of CWA, one can find a couple of lines, one of which (λ_1) is in the absorption maximum and the another (λ_2) is in the absorption band wing; therewith the absorption by the interfering gases is small and similar. The following atmospheric parameters were chosen: summer model of midlatitudes of the Northern Hemisphere, pressure of 1 atm, temperature of 296 K. The calculation results are given in Table 1.

Table 1. Chosen CO_2 lasing lines and absorption cross section σ of poison-gases

CWA	Lewisite	Sarin	Soman	Tabun	VX	Cyclosarin
Transition type and wavelength λ_1, μm	10P(30) 10.696	9P(44) 9.773	9P(40) 9.733	9P(22) 9.569	9P(16) 9.520	9P(26) 9.604
Transition type and wavelength λ_2, μm	10R(34) 10.158	9R(18) 9.282	9R(4) 9.367	9R(40) 9.174	10R(36) 10.115	9R(38) 9.183
$\sigma_1 \cdot 10^{-22}$, m^2	0.12	1.093	1.268	0.753	0.802	0.726
$\sigma_2 \cdot 10^{-22}$, m^2	0.007	0.037	0.068	0.068	0.055	0.027
$\sigma_{12} \cdot 10^{-22}$, m^2	0.113	1.056	1.2	0.685	0.747	0.699

The power of received backscattered radiation at the wavelengths λ_i ($i = 1, 2$) can be presented as[6]

$$P(R,\lambda_i) = \frac{c\,E\,K_1 K_2 \beta_\pi(\lambda_i)}{2}\left(\frac{A}{R^2}\right)G(R)\times$$

$$\times \exp 2\left\{-\int\left[\alpha_g(\lambda_i,z)+\alpha_a(\lambda_i,z)\right]dz\right\}, \quad (1)$$

where R is the distance; E is the lasing power; c is the light velocity; K_1 and K_2 are optical efficiencies of the lidar transmitter and receiver; A is the receiver's aperture area; $\beta_\pi(\lambda_i)$ is the backscattering volume factor of the atmospheric aerosol; α_g and α_a are the coefficients of molecular and aerosol attenuation, respectively; $G(R)$ is the lidar geometric factor.

The main limiting factor in the IR spectrum range is the detector shot noise. When detecting individual lidar signals, the signal-to-noise ratio ε is considered in the form[6]

$$\varepsilon = \frac{I_s}{\sqrt{2eB(I_s + I_b + I_d)}}, \quad (2)$$

where I_s is the signal current; I_b is the background current; I_d is the dark current; e is the electron charge; B is the width of detector transmission band. Equation (2) can be rewritten in the optical power units[6,7]:

$$\varepsilon = \frac{P_s}{\sqrt{\frac{2B(P_s + P_b)h\nu}{\eta} + BP_{ne}^2}}, \quad (3)$$

where P_s is the power of received signal; P_b is the power of background atmospheric radiation, incident on the detector area; η is the quantum efficiency of the detector; P_{ne} is the equivalent power of the detector noise; $h\nu$ is the quantum energy.

The equivalent noise power P_{ne} is expressed via the detector receiving area A_d and its detectability D^*:

$$P_{ne} = \sqrt{A_d}/D^*. \quad (4)$$

The detectability can be written as

$$D^* = \frac{\eta e}{h\nu}\sqrt{\frac{A_d}{2eI_d}}. \quad (5)$$

The power of background atmospheric radiation, incident on the detector area, has the form

$$P_b = K_2 B_a(\lambda)\Omega\Delta\lambda, \quad (6)$$

where $B_a(\lambda)$ is the background radiation brightness; Ω is the spatial visual angle of the receiver; $\Delta\lambda$ is the spectral width of the receiver's transmission band.

Calculation results

Consider the traditional scheme of biaxial CO_2 lidar. To simulate some attainable sensing range, lidar specifications, close to those given in Refs. 6 and 7, were taken. Thus, the transmitter specifications were

the following: radiation pulse energy $E = 1$ J; peak radiation pulse energy $P = 100$ MW; optical efficiency of beam former $K_1 = 0.7$; output beam diameter $2a_t = 100$ mm; divergence of the sensing beam $2\theta = 1$ mrad. The output aperture of sensing beams $2a_t$ was chosen to avoid the nonlinear radiation absorption by air. The radiation intensity should not exceed 0.8 MW/cm² [Ref. 7]. The lidar viewing angle 2φ is 1.5-time larger than the divergence of the sensing beam 2θ. The receiver has the following specifications: telescope aperture diameter $2a_r = 300$ mm; telescope focus length $f = 1500$ mm; viewing angle $2\varphi = 1.5$ mrad; optical efficiency $K_2 = 0.8$; transmission band width $B = 1$ MHz; distance between the transmitter and receiver axes $b_0 = 400$ mm, convergence angle of the axes $\psi = 0$ mrad.

As the detector in the lidar system receiver, a photodiode HgMnTe was considered, having the following parameters: detectability $D^* = 2\cdot10^{11}$ cm·Hz$^{1/2}$·W^{-1}; equivalent noise power $P_{ne} = 2.2\cdot10^{-13}$ W/Hz$^{1/2}$; size of the sensing area $d = 0.5$ mm; working temperature $T = 77$ K; spectral bandwidth $\Delta\lambda = 4$ μm [Ref. 9].

Consider the influence of different factors on the lidar sensing range in the surface air. Let the background concentrations of atmospheric gases and the parameters of surface layer of standard mid-latitude summer be the following: attenuation coefficient $\alpha_a = 0.03047$ km^{-1}, backscattering coefficient of atmospheric aerosol $\beta_\pi = 9.967\cdot10^{-5}$ km^{-1}·sr^{-1} [Ref. 10], background light brightness $B_a(\lambda) = 10^{-4}$ W/(cm²·sr·μm). The calculations were carried out for lines given in Table 1. Concentrations of warfare agents were: 5.5 ppm for tabun, 1.2 ppm for sarin; 0.43 ppm for soman, 0.84 ppm for VX, 14.05 ppm for lewisite, and 1.2 ppm for cyclosarin; these concentrations consist 10% of the threshold ones, resulting in the lethal dose at 1-min exposition.[1]

The calculated dependences of the signal-to-noise ratio ε on the range are shown in Fig. 1 for each CWA. The curves have been built for the case of single lidar echosignals. The limiting ranges of echolocation can be find from Fig. 1 at $\varepsilon = 1$: ~0.4 km for tabun; ~0.9 for lewisite; ~1 for sarin; ~1.5 for cyclosarin; ~1.8 for VX, and ~2.1 km for soman.

The diameter of the receiving mirror is very important for the lidar mobility and influences its mass-dimension parameters. Therefore, consider the influence of the receiving aperture area on the sensing range. When increasing the area of the receiving telescope, the recorded powers of both useful and background signals increase. According to the calculations, the increase of the area from 0.1 to 1 m² results in an insignificant increase in the sensing range, i.e., 19.8% for tabun; ~22.8 for lewisite; ~23.7 for sarin; ~25.5 for cyclosarin; ~26.7 for VX, and ~27.8% for soman.

Consider also the influence of the lidar's receiver viewing angle on the sensing range. Large viewing angles result in a decrease in measurement errors of gas contaminant concentrations in the atmosphere.[6]
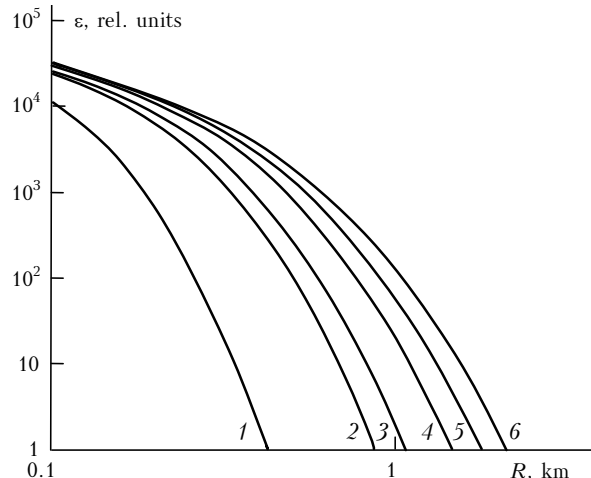
Fig. 1. Signal-to-noise ratio as a function of distance for tabun (*1*), lewisite (*2*), sarin (*3*), cyclosarin (*4*), VX (*5*), and soman (*6*) when recording single lidar echosignals.

When increasing the viewing angle, the echo-signal power is invariable, but the power of background radiation incident on the detector increases, which influences ε and the sensing range. The ratio between the lidar receiver viewing angle to the sensing beam divergence $\varphi/\theta = 1.5$ was supposed invariable. A weak dependence on the receiver viewing angle is observed in a range from 1 to 2–3 mrad, then the echolocation range decreases with an increase in viewing angle for all the gases under study.

Consider the influence of the laser power characteristics on the sensing range. Figure 2 shows the calculated dependences of the sensing range on the pulse power at $\varepsilon = 1$.
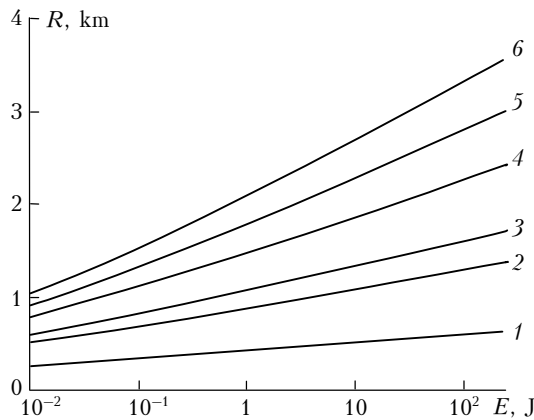
Fig. 2. Sensing range as a function of pulse power at $\varepsilon = 1$ for tabun (*1*), lewisite (*2*), sarin (*3*), cyclosarin (*4*), VX (*5*), and soman (*6*).

When increasing the power and peak power, the sensing range increases and the dependence is defined by the empirical equation

$$R_i(W) = A_i \ln(W) + B_i, \qquad (7)$$

where R_i is the echolocation range at $\varepsilon = 1$; $i = 1–6$ is the type of CWA. The values of numerical

coefficients A_i and B_i and their rms deviation σ_e for each CWA are given in Table 2.

**Table 2. Coefficients of Eq. (7) and rms deviations**

CWA	Lewisite	Sarin	Soman	Tabun	VX	Cyclosarin
A	0.089	0.113	0.259	0.038	0.213	0.167
B	0.897	1.093	2.139	0.434	1.831	1.502
σ_e	0.008	0.011	0.032	0.003	0.026	0.019

It follows from Fig. 2 that a 10-fold increase in the pulse power from 1 to 10 J results in an insignificant increase in sensing range, i.e., ~ 17.3% for tabun, ~ 19.5 for lewisite, ~ 20.1 for sarin, ~ 21.9 for cyclosarin, ~ 22.5 for VX, and ~ 23.5% for soman. Hence, there is no sense to improve laser power characteristics in comparison with those realized earlier in Refs. 7 and 8.

The performed calculations did not consider nonlinear absorption by the atmosphere, probable breakdown, and plasma formation at propagation of so high-power radiation. The accounting for these effects could result in a decrease in the threshold echolocation range, which is an additional illustration of the unnecessary use of large complex lasers with pulse powers of tens of joules.

Now consider the influence of the CWA concentration on the sensing range. In the above calculations, we used the value equal to 10% of the threshold concentrations of each gas under study. It is interesting to study the atmospheric sensing range at different values of the gas concentration. Figure 3 shows the calculated dependences of the sensing range on CWA concentrations in the atmosphere at $\varepsilon = 1$. It is evident that the sensing range increases with the decrease in the atmospheric attenuation.
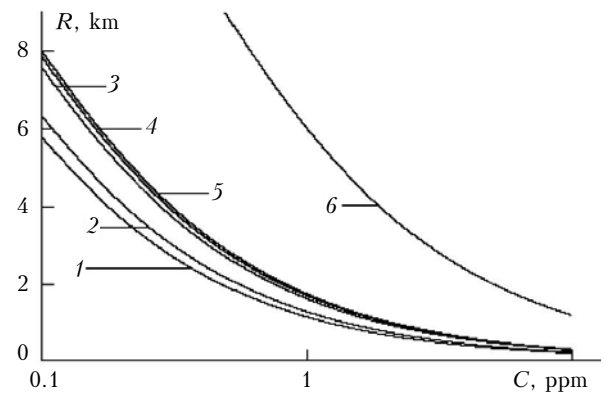
Fig. 3. Sensing range as a function of concentrations of soman (*1*), sarin (*2*), VX (*3*), tabun (*4*), cyclosarin (*5*), and lewisite (*6*) at $\varepsilon = 1$.

The 1-ppm concentration was chosen for all these gases without accounting for their toxic effect. The echolocation ranges for this concentration are given in Table 3.

Consider the atmospheric gas concentration measurement error. With neglect of changes of scattering properties in the spectral range of wavelength tuning from λ_1 to λ_2, the relative error δ_N can be written as[7]

$$\delta_N =$$

$$= \sqrt{\frac{\delta_1^2(R) + \delta_1^2(R+\Delta R) + \delta_2^2(R) + \delta_2^2(R+\Delta R)}{n\left(2\,\sigma_{12}\,C\Delta R\right)^2} + \delta_K^2 + \delta_F^2}, \ (8)$$

where σ_{12} is the differential absorption cross section; C is the gas concentration; δ_j are the relative measurement errors of lidar echo-signal powers, subscripts $j = 1, 2$ correspond to sensing at wavelengths λ_1 and λ_2; n is the number of radiation pulses; δ_K and δ_F are relative measurement errors of the differential absorption coefficient and the error due to the influence of interfering gases, they are systematic errors and do not correlate with detector noises.

Table 3. Sensing range at gas concentration $C = 1$ ppm

CWA	Soman	Sarin	VX	Tabun	Cyclosarin	Lewisite
Sensing range, km	~1.1	~1.2	~1.5	~1.6	~1.6	~5.9

Estimate the relative measurement error of CWA concentrations in the atmosphere according to Eq. (8), using the following values: C makes 10% of the threshold gas concentration; σ_{12} is from Table 1; $n = 10$; $\delta_K \sim 0.1$; $\delta_F \sim 0.1$;[6] spatial resolution $\Delta R = 100$ m.

At small distances, when lidar echo signals are recorded with a high signal-to-noise ratio, the measurement errors of CWA concentrations are determined by δ_K and δ_F. While increasing the sensing range, the measurement errors of echo-signal power increase. Maximum sensing ranges at $\delta_N = 1$ are ~ 0.3 km for tabun; ~ 0.8 for lewisite; ~ 1 for sarin; ~ 1.3 for cyclosarin; ~ 1.6 for VX, and ~ 1.9 km for soman.

Conclusion

Thus, based on the spectral dependence of absorption of the most common and dangerous CWA, we can conclude that differential CO_2-laser-based lidars are promising in detection of the gases. Couples of CO_2 lasing lines, optimal for sensing, have been chosen. The influence of different factors on the sensing range has been analyzed.

The sensing range has a nearly logarithmic dependence on pulse power. Further increase in laser pulse power in comparison with the realized parameters increases the sensing range insignificantly and has no sense.

Estimations of the relative measurement error of gas concentrations have shown that the CWA sensing is possible at their concentrations equal to 10% of the threshold ones, using aerosol backscattering within a radius of about 2 km depending on the CWA type.

References

1. M.E. Webber, M. Pushkarsky, and C.K. Patel, J. Appl. Phys. **97**, No. 11, 3101–3111 (2005).
2. O.G. Strukov, E.A. Fokin, V.A. Petrunin, I.V. Zavalishina, and Z.V. Vlasova, Khim. i Biolog. Bezopasnost, No. 5, 72–76 (2004).
3. V.A. Gorobets, V.O. Petukhov, S.Ya. Tochitskii, and V.V. Churakov, Quant. Electron. **25**, No. 5, 489–493 (1995).
4. S.F. Kol'yakov and L.P. Malyavkin, Sov. J. Quant. Electron. **18**, No. 1, 135–137 (1988).
5. L.S. Rothman, D. Jacquemart, A. Barbe, D.C. Benner, M. Birk, L.R. Brown, M.R. Carleer, C. Chackerian, Jr., K. Chance, L.H. Coudert, V. Dana, V.M. Devi, J.-M. Flaud, R.R. Gamache, A. Goldman, J.-M. Hartmann, K.W. Jucks, A.G. Maki, J.-Y. Mandin, S.T. Massie, J. Orphal, A. Perrin, M.A. Rinsland, M.A.H. Smith, J. Tennyson, R.N. Tolchenov, R.A. Toth, J. Vander Auwera, P. Varanasi, and G. Wagner, J. Quant. Spectrosc. and Radiat. Transfer **96**, No. 2, 139–204 (2005).
6. R.M. Measures, *Laser Remote Sensing* (John Wiley and Sons, New York, 1987).
7. M.V. Ivashchenko and I.V. Sherstov, Quant. Electron. **30**, 747–752 (2000).
8. Yu.M. Andreev, P.P. Geiko, and I.V. Sherstov, Proc. SPIE **3983**, 386–394 (1999).
9. A. Rogalskii, *IR Detectors* (Nauka, Novosibirsk, 2003), 636 pp.
10. G.M. Krekov and R.F. Rakhimov, *Optical Models of Atmospheric Aerosol* (Publishing House of Tomsk Branch of SB RAS, Tomsk, 1986), 283 pp.